JPE

A Simplified Carrier-Based Pulse-Width Modulation Strategy for Two-level Voltage Source Inverters in the Over-modulation Region

Feng Jing* and Feng-You He†

*School of Electrical and Power Engineering, China University of Mining and Technology, Xuzhou, China
†School of Electrical and Power Engineering, China University of Mining and Technology, Xuzhou, China

Abstract

In this study, a carrier-based pulse-width modulation (PWM) method for two-level voltage source inverters in the over-modulation region is proposed. Based on the superposition principle, the reference voltage vectors outside the linear modulation boundary are adjusted to relocate to the vector hexagon, while their fundamental magnitudes are retained. In accordance with the adjusted reference vector, the corresponding modulated waves are respectively deduced in over-modulation mode I and II to generate the gate signals of the power switches, guaranteeing the linearity of the fundamental output phase voltage in the over-modulation region. Moreover, due to the linear relationship between the voltage vector and the duty ratios, the complicated sector identification and holding angle calculation found in previous methods are avoided in the modulated wave synthesis, which provides great simplicity for the proposed carrier-based over-modulation strategy. Experimental results demonstrate the effectiveness and validity of the proposed method.

Key words: voltage-source inverter, pulse-width modulation, over-modulation region, carrier-based strategy.

I. INTRODUCTION

Pulse-Width Modulation (PWM) technology has been widely used in modern AC drive systems, which is directly related to the performance of the whole system. Most of the studies have been devoted to improving the performance of the PWM strategy in the linear modulation range [1-7]. However, in order to enhance the utilization rate of the dc-link voltage and to extend the adjustable speed range of AC motors, the operation ranges of the voltage-source inverters are often extended to the over-modulation region.

To obtain the linear fundamental output voltage of a voltage-source inverter VSI in the modulation region, many over-modulation algorithms from different perspectives have been discussed. The authors of [8-10] proposed a feed-forward over-modulation strategy for two-level inverters, which divided the over-modulation region into two zones. However, over-modulation strategy in [8-10] requires a large number of trigonometric function calculations and has to restore a lot of offset angles in the processors, which is difficult to realize using digital processors. Therefore, [11,12] proposed a linear approximation method to reduce the complexity of [8-10]. However, the fundamental output voltage is deceased. In addition, S. Bolognani proposed an over-modulation strategy based on reference angle correction and used offline

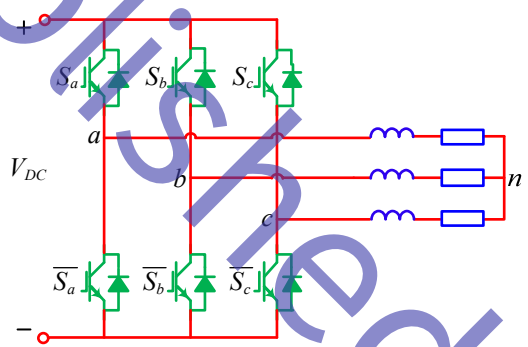

Fig. 1. Topology of two-level VSIs.

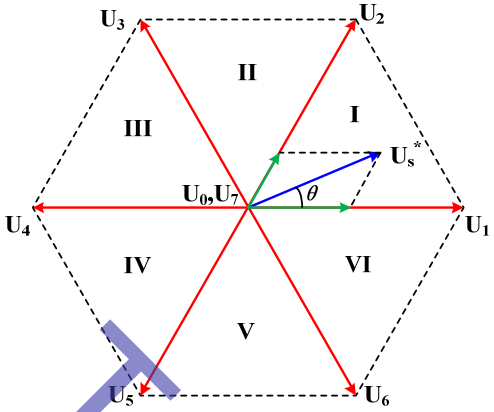

Fig. 2 Diagram of basic vectors and the synthesis approach in Sector I.

calculations to reduce the computation burden of the processors, but the wave quality of the output voltage is deteriorated [13]. In induction motor drive applications, the authors of [14-16] proposed a closed-loop compensation method based on back-EMF observation to increase the output stator voltage in the over-modulation region, which strongly relies on the precision of the parameter identification.

As described above, complicated procedures and calculations are required in the previous over-modulation strategies for two-level VSIs to maintain the linearity of the fundamental output voltage. As a result, high-performance processors are desired when the AC drives operate in the over-modulation range. This has the effect of increasing the cost of the drive systems. To solve this problem, [17] analyzed the relationship between the SVPWM strategy and the carrier-based PWM strategy. Then the authors proposed a carrier-based over-modulation algorithm to reduce the computational burden and to maintain the output wave quality. However, tedious anti-trigonometric function calculations are still required for obtaining the angle correction of the modulated waves, and sector identification also cannot be avoided. Therefore, improvement in the simplicity of the over-modulation strategy is still being sought.

This study aims at simplifying the over-modulation algorithm for two-level VSIs as well as maintaining the linearity of the fundamental output voltage and wave quality. First, the relationship between the duty ratios of the power switches and the duration times of the reference voltage vectors are analyzed. Then, space vector correction based on the superposition principle in the over-modulation region is introduced. As a result, the unified modulated waves in over-modulation modes I and II are derived for a carrier-based PWM strategy. It is found that the complicated calculations in the over-modulation region are greatly reduced by the proposed carrier-based PWM strategy, which is highly suitable for digital implementation. Finally, experimental results shows that the fundamental output voltage of an inverter using the proposed strategy always follows the reference one from the linear modulation range to the six-step mode. This demonstrats the validity and effectiveness of the proposed carrier-based over-modulation strategy.

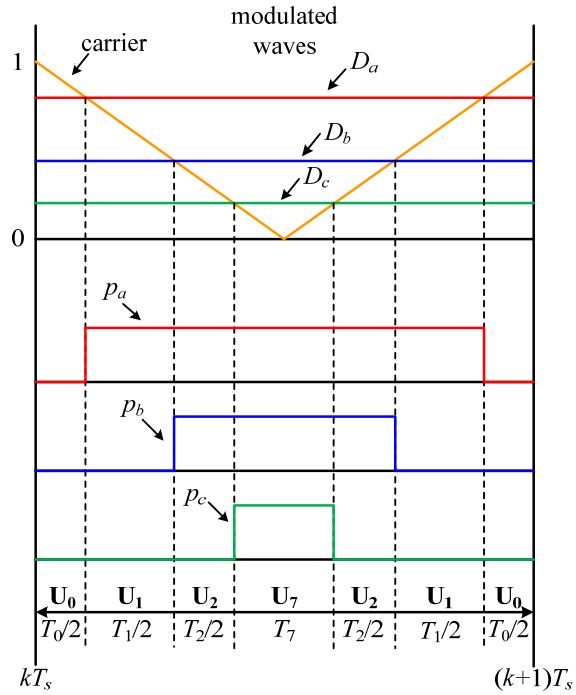

Fig. 3 Principle of the carrier-based PWM method.

II. PRINCIPLE OF THE CARRIER-BASED PWM METHOD FOR TWO-LEVEL VSIS

The topology of a two-level VSI is shown in Fig. 1. VDC is the DC-link voltage, and n is the neutral point of the AC side. The output voltage vector of the inverter can be described as:

$$\mathbf{U_s} = \begin{bmatrix} u_{an} \\ u_{bn} \\ u_{cn} \end{bmatrix} = \frac{V_{DC}}{3} \begin{bmatrix} 2p_a - p_b - p_c \\ 2p_b - p_a - p_c \\ 2p_c - p_a - p_b \end{bmatrix} \quad (1)$$

where p_a, p_b and p_c are switching functions defined as:

$$p_x = \begin{cases} 1, & S_x \ closed \\ 0, & \overline{S_x} \ closed \end{cases} \quad x = a, b, c \quad (2)$$

This represents the switching states of the six switches. By combining all of the possible switching states in (1), the eight basic vectors of the output voltage are shown in Fig. 2.

However, the mathematical model described in (1) is a high-frequency model, which is not applicable to AC drive control. Therefore, a low-frequency model described by the duty ratios of the power switches is established as:

$$\mathbf{U_s} = \begin{bmatrix} u_{an} \\ u_{bn} \\ u_{cn} \end{bmatrix} = \frac{V_{DC}}{3} \begin{bmatrix} 2D_a - D_b - D_c \\ 2D_b - D_a - D_c \\ 2D_c - D_a - D_b \end{bmatrix} \quad (3)$$

where D_a, D_b and D_c are the fundamental components of p_a, p_b, and p_c, respectively.

In digitaly controlled VSIs, three reference modulated waves

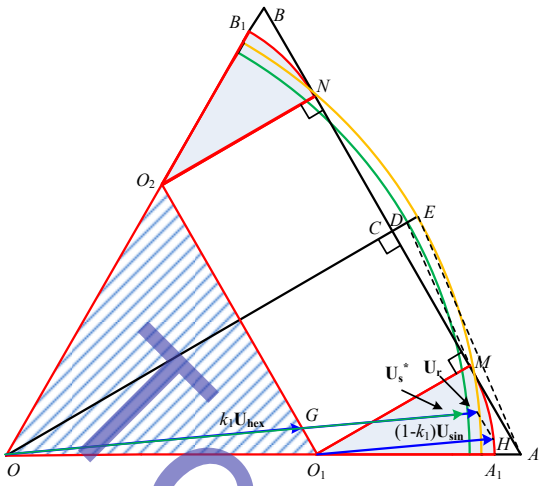

Fig. 4 Superposition principle in over-modulation mode I.

are compared with triangular carrier waves to generate the gate signals, as shown in Fig. 3. According to Fig. 3, it is clear that the modulated waves are the duty ratios of the power switches. Therefore, the calculation of the duty ratios is the key point in the carrier-based PWM method.

Suppose that $\mathbf{U_s}^*=[u_a^*, u_b^*, u_c^*]$ is located in Sector I ($\theta\in[0, \pi/6]$), as shown in Fig. 2. According to the principle of vector synthesis, the reference vector should be synthesized by the basic vectors $\mathbf{U_0}$, $\mathbf{U_1}$, $\mathbf{U_2}$, and $\mathbf{U_7}$. As a result, the duration time for each of the basic vectors can be obtained by:

$$\begin{cases} \mathbf{U_s}^* T_s = \mathbf{U_0} T_0 + \mathbf{U_1} T_1 + \mathbf{U_2} T_2 + \mathbf{U_7} T_7 \\ T_s = T_0 + T_1 + T_2 + T_7 \end{cases} \tag{4}$$

Accordingly, the duty ratios of S_a, S_b and S_c can be obtained as:

$$\begin{cases} D_a = (T_1 + T_2 + T_7)/T_s \\ D_b = (T_2 + T_7)/T_s \\ D_c = T_7/T_s \end{cases} \tag{5}$$

In the SVPWM method, the duration times of the zero vectors $\mathbf{U_0}$ and $\mathbf{U_7}$ should be equal to reduce the output voltage harmonics, e.g., $T_0=T_7$. By combining (4) and (5), the duty ratios can be expressed as:

$$\begin{cases} D_a = \frac{1}{2} + \frac{u_a^*/2 - u_c^*/2}{V_{DC}} = \frac{1}{2} + \frac{u_a^* - (u_a^* + u_c^*)/2}{V_{DC}} \\ D_b = \frac{1}{2} + \frac{-u_a^*/2 + u_b^* - u_c^*/2}{V_{DC}} = \frac{1}{2} + \frac{u_b^* - (u_a^* + u_c^*)/2}{V_{DC}} \\ D_c = \frac{1}{2} + \frac{-u_a^*/2 + u_c^*/2}{V_{DC}} = \frac{1}{2} + \frac{u_c^* - (u_a^* + u_c^*)/2}{V_{DC}} \end{cases} \tag{6}$$

In Sector I, the value of u_a^* is the maximum among u_a^*, u_b^* and u_c^*. Meanwhile, the value of u_c^* is the minimum among u_a^*, u_b^* and u_c^*. Therefore, the duty ratios in (6) can be rewritten as:

$$D_x = \frac{1}{2} + \frac{u_x^* - \left[\max(u_a^*, u_b^*, u_c^*) + \min(u_a^*, u_b^*, u_c^*)\right]/2}{V_{dc}}, \quad x = a, b, c \tag{7}$$

It should be noted that the conclusion in (7) can also be drawn when $\mathbf{U_s}^*$ lies in other sectors. In other words, (7) provides a direct approach to obtain unified modulated waves without complicated calculations. However, the modulated waves for two-level VSIs are only valid in the linear modulation range, while the carrier-based PWM method in the over-modulation region still remains to be explored.

III. SUPERPOSITION METHOD OF THE OVER-MODULATION STRATEGY

To identify the linear modulation range of PWM inverters, the modulation index m is defined as follows:

$$m = \frac{\pi |\mathbf{U_s}^*|}{2V_{DC}} \tag{8}$$

where $|\mathbf{U_s}^*|$ is the magnitude of the reference voltage vector.

The upper limit of the linear modulation range is when the modulation index is m=0.9069, which means the reference vector never exceeds the boundary of the hexagon in the vector plane. In the linear modulation region, the fundamental component of the output voltage is sinusoidal and undistorted. When m>0.9069, the output voltage of the inverter is distorted, which means that the fundamental component of the output voltage is not coincident with the reference one. According to the idea presented in [8-10], the over-modulation region can be divided into two parts: over-modulation mode I and over-modulation mode II. The critical condition between over-modulation modes I and II is that the trajectory of the actual reference voltage vector is the side of the hexagon in the vector plane, where the modulation index m is equal to 0.9523.

A. Over-modulation mode I (0.9069<m<0.9523)

Over-modulation mode I is operated when the magnitude of the desired voltage $\mathbf{U_s}^*$ is between two radii of an inscribed circle and a circumscribed circle of a hexagon. Therefore, the desired voltage vector sometimes exceeds the boundary of the hexagon. As a result, that the reference voltage vector needs to be properly adjusted to satisfy the voltage-second balance.

In [17], the over-modulation coefficient k_1 in over-modulation region I is defined as:

$$k_1 = \frac{m - 0.9069}{0.9523 - 0.9069} = \frac{m - 0.9069}{0.0457} \tag{9}$$

According to (9), when the reference voltage vector lies on the boundary of the linear modulation region, k_1=0; and when the trajectory of the reference vector is on the side of the hexagon, k_1=1.

Fig. 4 shows the adjusting process of the reference voltage vector. As shown in Fig. 4, the corresponding voltage vector $\mathbf{U_{sin}}$ of the inscribed circle lies on the boundary of the linear modulation region, which can be expressed as:

$$\mathbf{U_{sin}} = |OC| \cdot \mathbf{e}^{\mathbf{j}\theta} = \frac{V_{DC}}{\sqrt{3}} \mathbf{e}^{\mathbf{j}\theta} \tag{10}$$

Meanwhile, the voltage vector $\mathbf{U_{hex}}$ whose trajectory is the

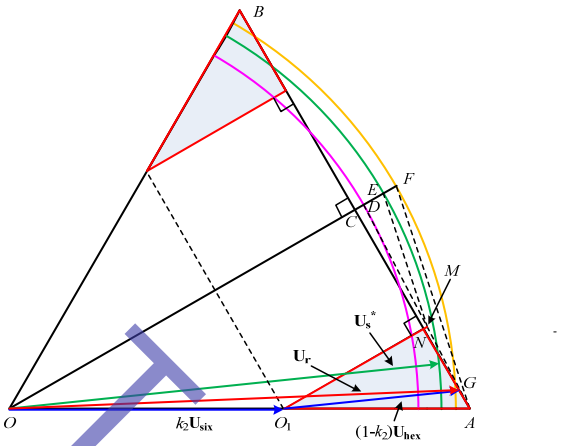

Fig. 5 The superposition principle in the over-modulation mode II.

side of the hexagon can be expressed as:

$$\mathbf{U_{hex}} = \frac{|OC|}{\cos(n\pi/6-\theta)}\mathbf{e^{j\theta}} = \frac{V_{DC}}{\sqrt{3}\cos(n\pi/6-\theta)}\mathbf{e^{j\theta}} \quad (11)$$

where n denotes the number of the corresponding sector. From [8], it is concluded that the fundamental magnitude of the vector $\mathbf{U_{hex}}$ is $0.6063V_{DC}$, which is equal to $|OE|$ as shown in Fig. 4. In addition, the magnitude of the desired voltage $\mathbf{U_s}^*$ is equal to $|OD|$, as shown in Fig. 4

As depicted in Fig. 4, $|DM|$ is paralleled to $|AE|$, which leads to:

$$\frac{|CM|}{|CA|} = \frac{|CD|}{|CE|} = k_1 \quad (12)$$

Then, according to a similar triangle principle, it is clear that $|OG|$ is equal to $k_1\mathbf{U_{hex}}$, and that $|O_1H|$ is equal to $(1\text{-}k_1)\mathbf{U_{sin}}$. The primary objective of the over-modulation strategy is to keep the fundamental magnitude of the actual output voltage coincident with the desired one. Therefore, based on the superposition principle in [17], it can be concluded that the adjusted reference vector $\mathbf{U_r}$ is composed of two parts: $\mathbf{U_{hex}}$ whose weight coefficient is k_1, and $\mathbf{U_{sin}}$ whose coefficient is $(1\text{-}k_1)$. Moreover, it is described as:

$$\mathbf{U_r} = k_1\mathbf{U_{hex}} + (1-k_1)\mathbf{U_{sin}} \quad (13)$$

The adjusted reference vector $\mathbf{U_r}$ in (13) has the same fundamental magnitude as that of $\mathbf{U_s}^*$. In addition, $\mathbf{U_r}$ is incapable of exceeding the boundary of in the hexagon, as shown in Fig. 4.

B. Over-modulation mode II (0.9523<m<1)

In over-modulation mode I, the angular velocity of the adjusted and actual voltage reference vectors is both the same and constant for each fundamental period. Under such a condition, a higher output phase voltage whose modulation index is above 0.9523 cannot be generated because there is no more surplus area to compensate the voltage loss.

When the modulation index is higher than 0.9523, the actual voltage reference vector is held at the vertex for a particular time to compensate the voltage-second loss. Then it moves along the side of the hexagon for the rest of the modulation period. In over-modulation mode II, the over-modulation coefficient is defined as:

$$k_2 = \frac{m-0.9523}{1-0.9523} = \frac{m-0.9523}{0.0477} \quad (14)$$

According to (14), when the trajectory of the actual reference vector is the hexagon vertex, namely the six-step mode, k_2=1. When the trajectory of the actual reference vector is the side of the hexagon, k_2=0. Fig. 5 shows the adjusting process of the reference voltage vector based on the superposition principle in [17]. The corresponding voltage vector $\mathbf{U_{six}}$ of the hexagon vertex can be expressed as:

$$\mathbf{U_{six}} = \frac{2V_{DC}}{3}\cdot\mathbf{e^{jn\pi/6}} \quad (15)$$

where n denotes the number of the sector in which the reference voltage vector lies.

In over-modulation mode II, the actual voltage vector $\mathbf{U_r}$ lies between $\mathbf{U_{hex}}$ and $\mathbf{U_{six}}$. As shown in Fig. 5, $|OC|$ denotes the fundamental magnitude of the hexagon vector $\mathbf{U_{hex}}$, $|OD|$ denotes the magnitude of the desired voltage vector $\mathbf{U_s}^*$, and $|OE|$ denotes the fundamental magnitude of the hexagon vertex vector $\mathbf{U_{six}}$. As shown in Fig. 5, $|DM|$ is paralleled to $|AE|$, and $|O_1G|$ is paralleled to $|ON|$. Therefore, it can be concluded that:

$$\frac{|OO_1|}{|OA|} = \frac{|CN|}{|CA|} = \frac{|DM|}{|DA|} = \frac{|DE|}{|DF|} = k_2 \quad (16)$$

Then, it is clear that $|OO_1|$ is equal to $k_2\mathbf{U_{six}}$, and $|O_1G|$ is equal to $(1\text{-}k_2)\mathbf{U_{hex}}$. Similar to that in over-modulation mode I, $\mathbf{U_r}$ is also composed of two parts: a $\mathbf{U_{six}}$ whose weight coefficient is k_2, and a $\mathbf{U_{hex}}$ whose weight coefficient is $(1\text{-}k_2)$. Therefore, it can be concluded that:

$$\mathbf{U_r} = k_2\mathbf{U_{six}} + (1-k_2)\mathbf{U_{hex}} \quad (17)$$

According to the superposition principle, the adjusted reference vector $\mathbf{U_r}$ in (17) has the same fundamental magnitude as that of $\mathbf{U_s}^*$ in over-modulation mode II. As in over-modulation mode I, $\mathbf{U_r}$ is also incapable of exceeding the boundary in the hexagon, as shown in Fig. 5.

IV. SIMPLIFIED CARRIER-BASED PWM STRATEGY IN THE OVER-MODULATION REGION

According to the conclusion drawn in Section III, the reference voltage vector in the over-modulation region is adjusted to keep lying in the hexagon with the same fundamental magnitude. The following procedure is to derive the related modulation functions to generate the pulses for the power switches.

A. The carrier-based PWM method in over-modulation mode I

In over-modulation mode I, the adjusted reference voltage vector is composed of $\mathbf{U_{sin}}$ and $\mathbf{U_{hex}}$, as depicted in (13). According to the principle of the carrier-based PWM method shown in (7), the duty ratios for the adjusted reference voltage vector $\mathbf{U_r}$ can be expressed as:

$$D_{r\_x} = (1-k_1)\left(D_{\sin\_x} - \frac{1}{2}\right) + k_1\left(D_{hex\_x} - \frac{1}{2}\right) + \frac{1}{2} = (1-k_1)D_{\sin\_x} + k_1 D_{hex\_x}, \quad x = a,b,c \tag{18}$$

where D_{sin_x} and D_{hex_x} denote the duty ratios for the vectors $\mathbf{U_{sin}}$ and $\mathbf{U_{hex}}$, respectively. Then, it is clear that the duty ratios of the vectors $\mathbf{U_{sin}}$ and $\mathbf{U_{hex}}$ are desiderated for the calculation of the modulated waves in over-modulation mode I.

As depicted in Fig. 4, there is no phase difference between the actual voltage reference vector $\mathbf{U_r}$ and the desired voltage reference vector $\mathbf{U_s}^*$. This is due to the fact that $\mathbf{U_{sin}}$ and $\mathbf{U_{hex}}$ have the same phase as $\mathbf{U_s}^*$. Therefore, it is clear that:

$$\mathbf{U_{sin}} = \frac{\sqrt{3}V_{DC}}{3\left|\mathbf{U_s^*}\right|}\mathbf{U_s^*} \tag{19}$$

$$\mathbf{U_{hex}} = k\mathbf{U_s^*} \tag{20}$$

where k is the coefficient describing the length difference between $\mathbf{U_{hex}}$ and $\mathbf{U_s}^*$. Since the trajectory of $\mathbf{U_{hex}}$ is the side of the hexagon, the length of $\mathbf{U_{hex}}$ is time variant. Thus, k is also time variant. By substituting (19) into (7), the duty ratio for $\mathbf{U_{sin}}$ can be derived as (21).

$$\begin{aligned} D_{\sin\_x} &= \frac{1}{2} + \left\{ \frac{\sqrt{3}V_{DC}}{3\left|\mathbf{U_s^*}\right|}u_x^* - \frac{1}{2}\max\left(\frac{\sqrt{3}V_{DC}}{3\left|\mathbf{U_s^*}\right|}u_a^*, \frac{\sqrt{3}V_{DC}}{3\left|\mathbf{U_s^*}\right|}u_b^*, \frac{\sqrt{3}V_{DC}}{3\left|\mathbf{U_s^*}\right|}u_c^* \right) - \right. \\ &\left. \frac{1}{2}\min\left(\frac{\sqrt{3}V_{DC}}{3\left|\mathbf{U_s^*}\right|}u_a^*, \frac{\sqrt{3}V_{DC}}{3\left|\mathbf{U_s^*}\right|}u_b^*, \frac{\sqrt{3}V_{DC}}{3\left|\mathbf{U_s^*}\right|}u_c^* \right) \right\} \Big/ V_{DC} \\ &= \frac{1}{2} + \frac{\sqrt{3}\left[u_x^* - \frac{1}{2}\max\left(u_a^*, u_b^*, u_c^*\right) - \frac{1}{2}\min\left(u_a^*, u_b^*, u_c^*\right) \right]}{3\left|\mathbf{U_s^*}\right|}, \\ & x = a,b,c \end{aligned} \tag{21}$$

When the voltage vector moves along the side of the hexagon, it is clear that the voltage vector $\mathbf{U_{hex}}$ is synthesized by two non-zero basic vectors. In other words, the duration times of the zero vectors $\mathbf{U_0}$ and $\mathbf{U_7}$ are null during each switching period. As a result, the duty ratio for the maximum phase voltage of the vector $\mathbf{U_{hex}}$ is always equal to 1, which can be expressed as:

$$\max\left(D_{hex\_a}, D_{hex\_b}, D_{hex\_c}\right) = 1 \tag{21}$$

By substituting (20) into (7), the duty ratios for $\mathbf{U_{hex}}$ can be expressed as:

$$\begin{aligned} D_{hex\_x} &= \frac{1}{2} + k\left(D_x - \frac{1}{2}\right) \\ &= \frac{1}{2} + k\left[u_x^* - \frac{1}{2}\max\left(u_a^*, u_b^*, u_c^*\right) - \right. \\ &\left. \frac{1}{2}\min\left(u_a^*, u_b^*, u_c^*\right) \right] \Big/ V_{DC}, \quad x = a,b,c \end{aligned} \tag{22}$$

From (23), it is clear that the maximum duty ratio can be expressed as:

$$\begin{aligned} &\max\left(D_{hex\_a}, D_{hex\_b}, D_{hex\_c}\right) \\ &= \frac{1}{2} + k\left[\max\left(u_a^*, u_b^*, u_c^*\right) - \frac{1}{2}\max\left(u_a^*, u_b^*, u_c^*\right) - \right. \\ &\left. \frac{1}{2}\min\left(u_a^*, u_b^*, u_c^*\right) \right] \Big/ V_{DC} \\ &= \frac{1}{2} + \frac{k\left[\max\left(u_a^*, u_b^*, u_c^*\right) - \min\left(u_a^*, u_b^*, u_c^*\right) \right]}{2V_{DC}} \end{aligned} \tag{23}$$

By substituting (24) into (22), the time-variant coefficient k can be derived as:

$$k = \frac{V_{DC}}{\max\left(u_a^*, u_b^*, u_c^*\right) - \min\left(u_a^*, u_b^*, u_c^*\right)} \tag{24}$$

By substituting (25) into (23), the duty ratios for $\mathbf{U_{hex}}$ can be presented by:

$$D_{hex\_x} = \frac{1}{2} + \frac{u_x^* - \frac{1}{2}\max\left(u_a^*, u_b^*, u_c^*\right) - \frac{1}{2}\min\left(u_a^*, u_b^*, u_c^*\right)}{\max\left(u_a^*, u_b^*, u_c^*\right) - \min\left(u_a^*, u_b^*, u_c^*\right)}, \quad x = a,b,c \tag{25}$$

When the duty ratios for $\mathbf{U_{sin}}$ and $\mathbf{U_{hex}}$ are obtained, the modulation functions in over-modulation mode I can be derived by substituting (21) and (26) into (18):

$$\begin{aligned} D_{r\_x} &= (1-k_1)D_{\sin\_x} + k_1 D_{hex\_x} \\ &= \frac{1}{2} + \frac{\sqrt{3}(1-k_1)\left[u_x^* - \frac{1}{2}\max\left(u_a^*, u_b^*, u_c^*\right) - \frac{1}{2}\min\left(u_a^*, u_b^*, u_c^*\right) \right]}{3\left|\mathbf{U_s^*}\right|} + \\ &\frac{k_1\left[u_x^* - \frac{1}{2}\max\left(u_a^*, u_b^*, u_c^*\right) - \frac{1}{2}\min\left(u_a^*, u_b^*, u_c^*\right) \right]}{\max\left(u_a^*, u_b^*, u_c^*\right) - \min\left(u_a^*, u_b^*, u_c^*\right)} \\ &= \frac{1}{2} + \left[\frac{\sqrt{3}(1-k_1)}{3\left|\mathbf{U_s^*}\right|} + \frac{k_1}{\max\left(u_a^*, u_b^*, u_c^*\right) - \min\left(u_a^*, u_b^*, u_c^*\right)} \right] \cdot \\ &\left[u_x^* - \frac{1}{2}\max\left(u_a^*, u_b^*, u_c^*\right) - \frac{1}{2}\min\left(u_a^*, u_b^*, u_c^*\right) \right], \quad x = a,b,c \end{aligned} \tag{26}$$

The carrier-based PWM method in over-modulation mode I is based on (27), by which the modulation pulses can be easily obtained.

B. The carrier-based PWM method in over-modulation mode II

In over-modulation mode II, the actual voltage reference vector and the desired voltage reference vector are no longer synchronous, as shown in Fig. 5. Because of the angle difference between $\mathbf{U_s}^*$ and $\mathbf{U_r}$, the calculation of the duration times of the basic vectors becomes tedious and complicated. However, the adjusted voltage vector $\mathbf{U_r}$ still lies in the hexagon based on the superposition principle. Therefore, the carrier-based PWM method is still applicable in over-modulation mode II.

According to (17), the duty ratios for $\mathbf{U_r}$ in over-modulation mode II can be expressed as:

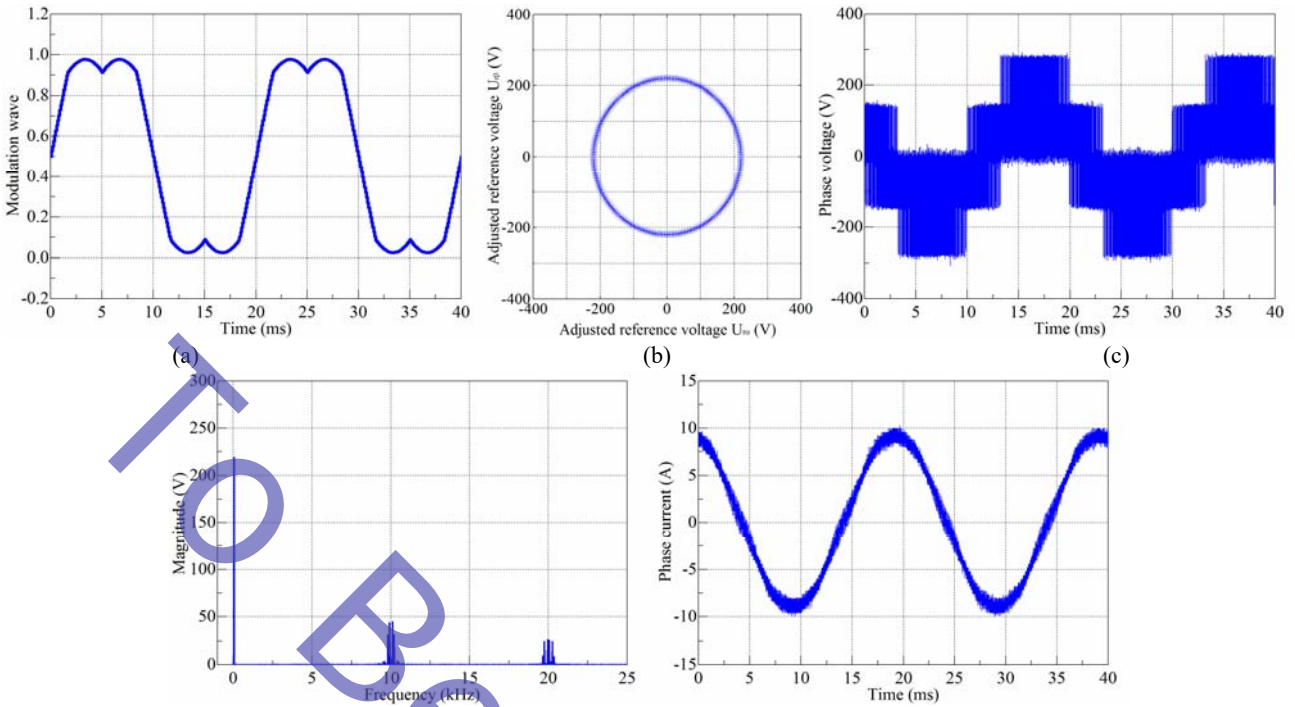

Fig. 6 Experimental results at the linear modulation region (m=0.8693): (a) modulated wave; (b) trajectory of the adjusted reference vector; (c) output phase voltage; (d) FFT analysis result of the phase voltage; (e) output phase current.

$$D_{r\_x} = (1-k_2)\left(D_{hex\_x} - \frac{1}{2}\right) + k_2\left(D_{six\_x} - \frac{1}{2}\right) + \frac{1}{2} = (1-k_2)D_{hex\_x} + k_2 D_{six\_x}, \quad x = a,b,c \tag{27}$$

The duty ratio D_{hex} for the voltage vector $\mathbf{U_{hex}}$ in (28) can be obtained by (26). Then, the duty ratio D_{six} for the voltage vector of the hexagon vertex is desired. Actually, the voltage vector $\mathbf{U_{six}}$ is operated in the six-step mode, which is composed of six non-zero basic voltage vectors, namely $\mathbf{U_1}$(100), $\mathbf{U_2}$(110), $\mathbf{U_3}$(010), $\mathbf{U_4}$(011), $\mathbf{U_5}$(001) and $\mathbf{U_6}$(101). In the six-step mode, the power switches have only one state during a switching period. Moreover, when the reference phase voltage is positive, the corresponding power switch is always turned-on. When the reference phase voltage is negative, the corresponding power switch is always turned-off. Therefore, the modulated waves for the vector $\mathbf{U_{six}}$ can be easily expressed as:

$$D_{six\_x} = \frac{1}{2} sign\left(u_x^*\right) + \frac{1}{2}, \quad x = a,b,c \tag{28}$$

where:

$$sign(u_x^*) = \begin{cases} 1, & u_x^* > 0 \\ -1, & u_x^* < 0 \end{cases} \tag{29}$$

By substituting (26) and (29) into (28), the modulation functions in over-modulation mode II can be expressed as:

$$D_{r\_x} = (1-k_2)D_{hex\_x} + k_2 D_{six\_x} = \frac{1}{2} + \frac{(1-k_2)\left[u_x^* - \frac{1}{2}\max\left(u_a^*, u_b^*, u_c^*\right) - \frac{1}{2}\min\left(u_a^*, u_b^*, u_c^*\right)\right]}{\max\left(u_a^*, u_b^*, u_c^*\right) - \min\left(u_a^*, u_b^*, u_c^*\right)} + \frac{k_2}{2} sign\left(u_x^*\right), \quad x = a,b,c \tag{30}$$

From (31), it is clear that the complicated calculations for the holding angle are avoided, while only a few simple calculations and logical operations are required. It is concluded that the proposed carrier-based PWM method in the over-modulation region is very simple and effective. In addition, if the modulation index is larger than 1, this means that the linearity of the fundamental components can no longer be guaranteed. In this case, the VSI is operated in the six-step mode, whose modulated waves should be in accordance with (29).

TABLE I

PARAMETERS OF THE TEST BENCH

DC-link voltage	400 V
Fundamental frequency	50 Hz
Switching frequency	10 kHz
Load resistance	22 Ω
Load inductance	3 mH

V. EXPERIMENTAL RESULTS

To verify the proposed over-modulation algorithm, a commercial two-level VSI test bench was built with a digital

signal processor (DSP) TMS320F2808. A three-phase series R-L load is connected to the output side of the VSI. The parameters of the test bench are shown in Table I.

The carrier-based PWM method is first tested in the linear modulation region. The magnitude of the reference voltage vector is set to 220 V, whose modulation index is equal to 0.8639. The experimental results are shown in Fig. 6. The maximum value of the modulated wave is less than 1, representing that the reference voltage vector is located in the linear modulation region. As a result, the trajectory of the reference vector is circular, as shown in Fig. 6(b). The harmonics of the output voltage only contain the high frequency components around the switching frequency, as shown in Fig. 6(d). Consequently, the output phase current is almost sinusoidal and without low frequency harmonics.

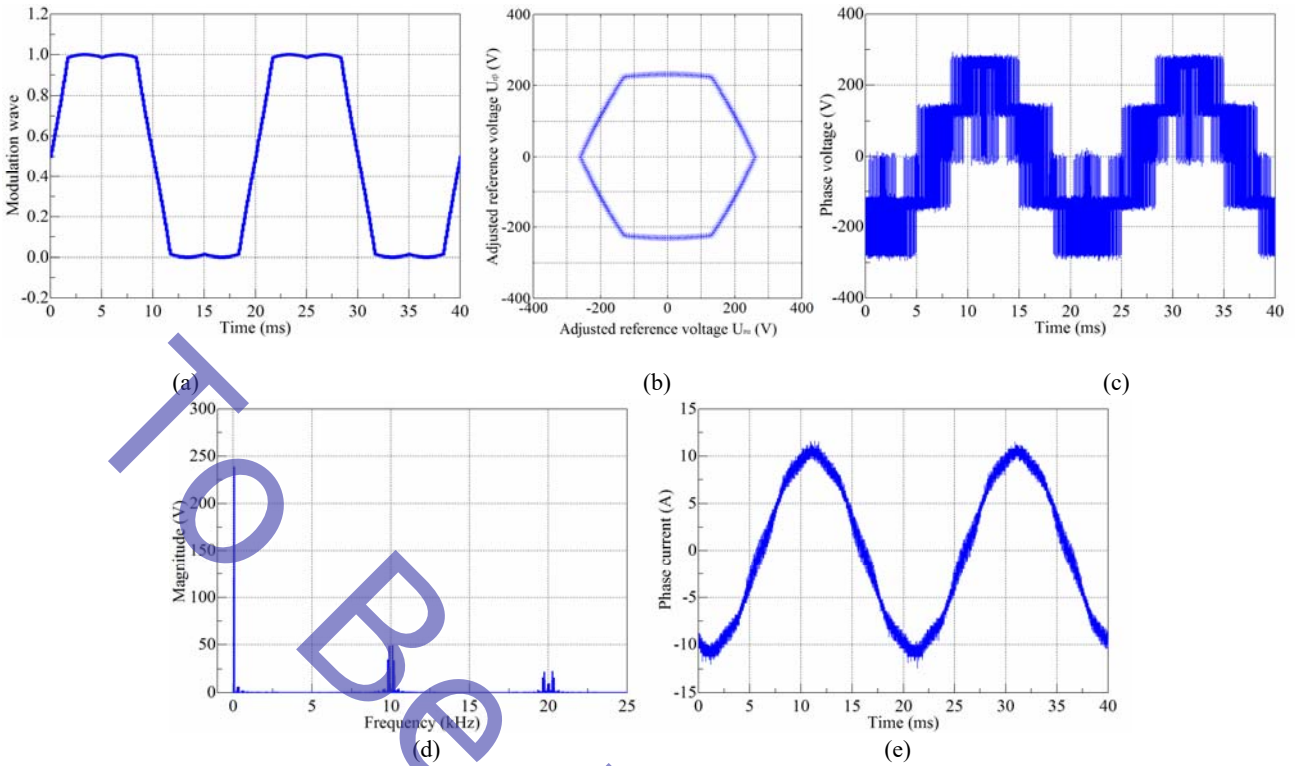

Fig. 7 Experimental results in over-modulation mode I (m=0.9425): (a) modulated wave; (b) trajectory of the adjusted reference vector; (c) output phase voltage; (d) FFT analysis result of the phase voltage; (e) output phase current.

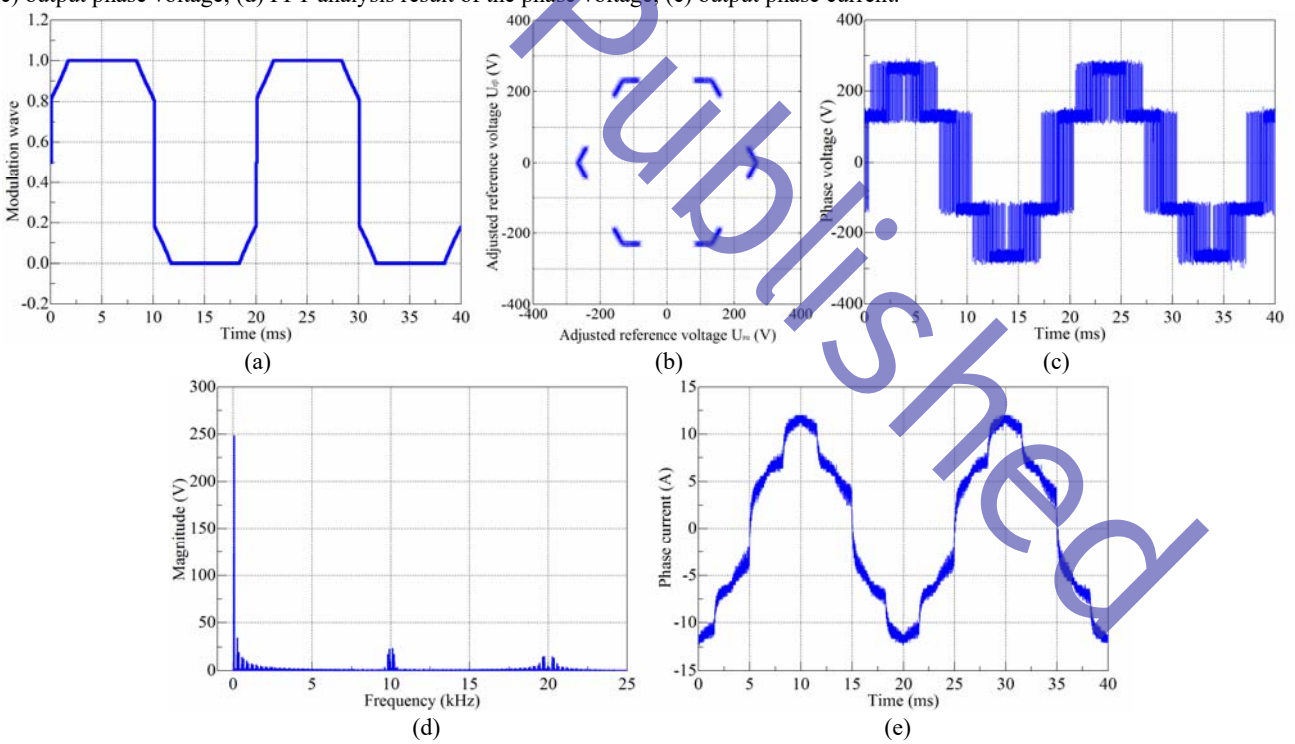

Fig. 8 Experimental results in over-modulation mode II (m=0.9817): (a) modulated wave; (b) trajectory of the adjusted reference vector; (c) output phase voltage; (d) FFT analysis result of the phase voltage; (e) output phase current.

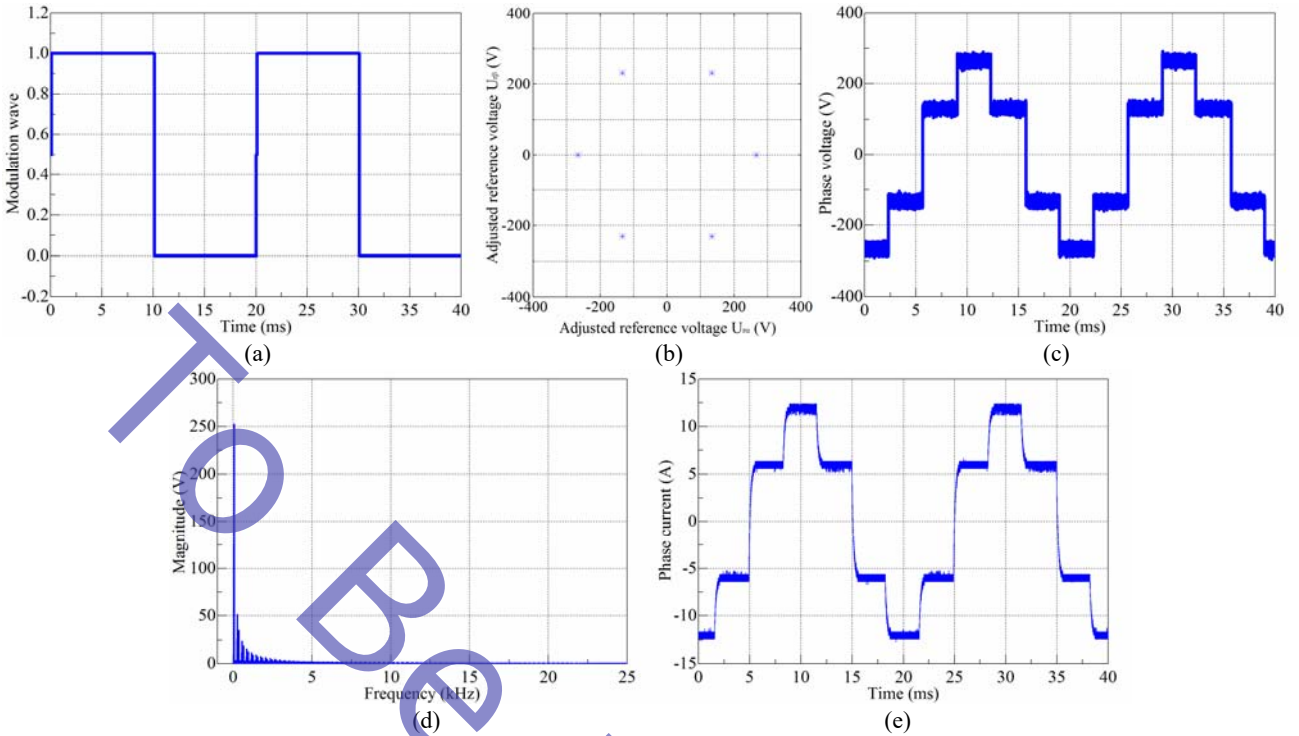

Fig. 9 Experimental results in six-step mode (m=1.021): (a) modulated wave; (b) trajectory of the adjusted reference vector; (c) output phase voltage; (d) FFT analysis result of the phase voltage; (e) output phase current.

Then, the magnitude of the reference voltage vector is set to 240 V, whose modulation index is 0.9425. In this case, the VSI is operated in over-modulation mode I. Experimental results in the over-modulation mode I are shown in Fig. 7. The peak value of the modulated wave is equal to 1. This represents that the VSI is operated in the over-modulation region. In addition, the trajectory of the adjusted reference voltage vector is not circular, but nearly a hexagon. Consequently, a few low frequency harmonics are injected into the output phase voltage, as shown in Fig. 7(d). Therefore, the output current is also polluted by low frequency harmonics.

When the magnitude of the reference voltage vector is set to 250 V, the VSI is operated in over-modulation mode II, whose modulation index is 0.9817. When m increases further, the points of the modulated wave whose value is 1 increase, as shown in Fig. 8(a). The trajectory of the adjusted reference vector consists of several points at around six vertexes of the hexagon. Consequently, the low frequency harmonics in the output phase voltage and current become severe, as shown in Fig. 8(d) and (e).

When the magnitude of the reference voltage vector continues to increase to 260 V, the modulation index is bigger than 1, which represents that the VSI is operated in the six-step mode. In this case, the fundamental component of the output phase voltage is not able to follow the reference one, and the trajectory of the adjusted voltage vector is the six vertexes of the hexagon, as shown in Fig. 9(b). The high-frequency switching actions of the power switches totally vanish in the six-step mode. This is due to the fact that the value of the modulated wave is either 1 or 0 along the half fundamental period. Thus, the high-frequency switching harmonics in the output voltage and current are eliminated, as shown in Fig. 9(d) and (e).

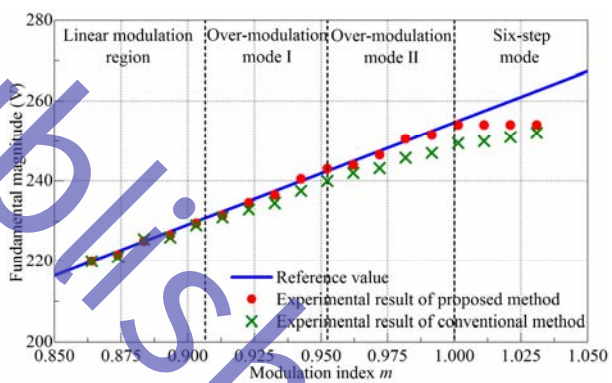

Fig. 10 Experimental results of the fundamental magnitude of the output phase voltage.

To verify the output linearity of the proposed carrier-based method, a comparison between the reference fundamental magnitudes and the experimental results is conducted. As shown in Fig. 10, in the linear modulation region, the experimental results are well coincident with the reference ones. Moreover, in the over-modulation region, the fundamental magnitude of the output phase voltage is also consistent with the desired magnitude, which represents the superior output linearity of the proposed over-modulation strategy. When the

modulation index is beyond 1, it is clear the VSI is operated in the six-step mode, and that the output voltage is restricted.

VI. Conclusions

This study gives sufficient insight into over-modulation strategies for two-level voltage-source inverters. Due to the complexity of SVPWM in the over-modulation region, a carrier-based PWM method is proposed to generate the corresponding gate signals. Based on the superposition principle, the reference voltage vectors in over-modulation mode I are decomposed into the vector $\mathbf{U}_{hex}$ along the side of the hexagon and the vector $\mathbf{U}_{sin}$ along the side of the inscribed circle. The reference voltage vectors in over-modulation II are decomposed into the vector $\mathbf{U}_{hex}$ along the side of the hexagon and the vector $\mathbf{U}_{six}$ of the hexagon vertexes. In this way, the reference vectors outside the modulation range are adjusted to be located in the hexagon, while the fundamental magnitudes are retained. Then, the unified modulated waves in over-modulation modes I and II are deduced. Moreover, the complicated procedures of sector identification and holding angle calculation are avoided in the proposed carrier-based over-modulation strategy, which greatly reduces the computational burden of the digital processor. Experimental results demonstrate that the fundamental magnitudes of the output phase voltages are well coincident with the reference ones in the over-modulation region, which validates the excellent simplicity and output linearity of the proposed carrier-based over-modulation strategy.

Acknowledgment

This work is supported by National Key Research and Development Program of China (2016YFC0600906).

References

[1] D. Casadei, G. Serra, A. Tani, et al. “Theoretical and experimental analysis for the RMS current ripple minimization in induction motor drives controlled by SVM technique,” *IEEE Trans. Ind. Electron.*, Vol. 51, No. 5, pp. 1056-1065, Oct. 2004.

[2] G. Narayanan and V. T. Ranganathan, “Analytical evaluation of harmonic distortion in PWM AC drives using the notion of stator flux ripple,” *IEEE Trans. Power Electron.*, Vol. 20, No. 2, pp. 466-474, Mar. 2005.

[3] A. M. Hava and E. Un, “Performance analysis of reduced common-mode voltage PWM methods and comparison with standard PWM methods for three-phase voltage-source inverters,” *IEEE Trans. Power Electron.*, Vol. 24, No. 1, pp. 241-252, Jan. 2009.

[4] K. Basu, J. Prasad and G. Narayanan, “Minimization of torque ripple in PWM AC drives,” *IEEE Trans. Ind. Electron.*, Vol. 56, No. 2, pp. 553-558, Feb. 2009.

[5] K. Basu, J. S. S. Prasad, G. Narayanan, H. K. Krishnamurthy, and R. Ayyanar, “Reduction of torque ripple in induction motor drives using an advanced hybrid PWM technique,” *IEEE Trans. Ind. Electron.*, Vol. 57, No. 6, pp. 2085-2091, Jun. 2010.

[6] C. C. Hou, C. C. Shih, P. T. Cheng, and A. M. Hava, “Common-Mode Voltage Reduction Pulsewidth Modulation Techniques for Three-Phase Grid-Connected Converters,” *IEEE Trans. Power Electron.*, Vol. 28, No. 4, pp. 1971-1979, Apr. 2013.

[7] V. S. S. P. Hari and G. Narayanan, “Theoretical and experimental evaluation of pulsating torque produced by induction motor drives controlled with advanced bus-clamping pulsewidth modulation,” *IEEE Trans. Ind. Electron.*, Vol. 63, No. 3, pp. 1404-1413, Mar. 2016.

[8] J. Holtz, W. Lotzkat and A. M. Khambadkone, “On continuous control of PWM inverters in the overmodulation range including the six-step mode,” *IEEE Trans. Power Electron.*, Vol. 8, No. 4, pp. 546-553, Oct. 1993.

[9] V. Kaura and V. Blasko, “A new method to extend linearity of a sinusoidal PWM in the overmodulation region,” *IEEE Trans. Ind. Appl.*, Vol. 32, No. 5, pp. 1115-1121, Sep./Oct. 1996.

[10] R. J. Kerkman, D. Leggate, B. J. Seibel, and T. M. Rowan, “Operation of PWM voltage source-inverters in the overmodulation region,” *IEEE. Tran. Ind. Electron.*, Vol. 43, No. 1, pp. 132-141, Feb. 1996.

[11] D. Lee and G. Lee, “Linear control of inverter output voltage in overmodulation,” *IEEE Trans. Ind. Electron.*, Vol. 44, No. 4, pp. 590-592, Aug. 1997.

[12] D. Lee and G. Lee, “A novel overmodulation technique for space-vector PWM inverters,” *IEEE Trans. Power Electron.*, Vol. 13, No. 6, pp. 1144-1151, Nov. 1998.

[13] S. Bolognani and M. Zigliotto, “Novel digital continuous control of SVM inverters in the overmodulation range,” *IEEE Trans. Ind. Appl.*, Vol. 33, No. 2, pp. 525-530, Mar./Apr. 1997.

[14] G. Narayanan and V. T. Ranganathan, “Extension of operation of space vector PWM strategies with low switching frequencies using different overmodulation algorithms,” *IEEE Trans. Power Electron.*, Vol. 17, No. 5, pp. 788-798, Sep. 2002.

[15] A. Tripathi, A. M. Khambadkone and S. K. Panda, “Stator flux based space-vector modulation and closed loop control of the stator flux vector in overmodulation into six-step mode,” *IEEE Trans. Power Electron.*, Vol. 19, No. 3, pp. 775-782, May 2004.

[16] A. Tripathi, A. M. Khambadkone and S. K. Panda, “Direct method of overmodulation with integrated closed loop stator flux vector control,” *IEEE Trans. Power Electron.*, Vol. 20, No. 5, pp. 1161-1168, Sep. 2005.

[17] H. Fang, X. Feng, W. Song, X. Ge, and R. Ding, “Relationship between two-level space-vector pulse-width modulation and carrier-based pulsewidth modulation in the over-modulation region,” *IET Power Electron.*, Vol. 7, No. 1, pp. 189-199, Jan. 2014

Feng Jing was born in Anhui, China. She received her B.S. degree in Electrical Engineering from the Anhui University of Science and Technology, Anhui, China, in 2006. She is presently working towards her Ph.D. degree in the School of Electrical and Power Engineering, China University of Mining and Technology, Xuzhou, China. Her current research interests include the modeling and modulation of power electronics converters.

Feng-You He was born in Zhangjiakou, Hebei, China, in 1963. He received his B.S. degree in Automation, and his M.S. and Ph.D. degrees in Power Electronics and Power Drives from the China University of Mining and Technology, Xuzhou, China, in 1984, 1992 and 1995, respectively. Since 1984, he has been with the Department of Information and Electrical Engineering, China University of Mining and Technology, where he is presently working as a Professor. His current research interests include the improvement of inverters, the advanced control of electrical machines, and power electronics.